The principles underlying the use of powder diffraction data in solving pharmaceutical crystal structures

Article

Accepted Version

ACCEPTED

The principles underlying the use of powder diffraction data in solving pharmaceutical crystal structures

Kenneth Shankland,[a]* Mark J. Spillman,[a] Elena A. Kabova,[a] David S. Edgeley[a] and Norman Shankland[b]

[a]School of Pharmacy, Univerity of Reading, Whiteknights Campus, Reading, Berkshire RG6 6AD, England, and [b]CrystallografX Limited, 2 Stewart Street, Milngavie G62 6BW, Scotland
Correspondence e-mail: k.shankland@reading.ac.uk

Solving pharmaceutical crystal structures from powder diffraction data is discussed in terms of the methodologies that have been applied and the complexity of the structures that have been solved. The principles underlying these methodologies are summarized and representative examples of polymorph, solvate, salt and cocrystal structure solutions are provided, together with examples of some particularly challenging structure determinations.

Keywords: pharmaceuticals; crystal structure; powder diffraction.

1. Introduction

The investigation of crystalline materials is an integral part of the processes involved in bringing a new drug to market. Numerous techniques, including thermal and spectroscopic methods, are available to the solid-state analyst; for a comprehensive review of the relative merits and frequency of use of such techniques, see Chieng et al. (2011). Organic small-molecule drugs are almost invariably crystalline and so it is perhaps unsurprising that powder X-ray diffraction (PXRD) is the most frequently used analytical method.

The versatility of PXRD data is demonstrated by its use throughout the different stages of the drug manufacturing lifecycle (Ivanisevic et al., 2010; Randall et al., 2010; Brittain, 2001). Its importance as a 'fingerprint' with which to identify specific crystallographic phases is evidenced by its central role in high-throughput physical form screening and its use (either in diagrammatic form, or as a series of reflection positions) in patents designed to protect physical forms. These aspects have been reviewed comprehensively elsewhere (Morissette et al., 2004; Florence, 2009; Lemmerer et al., 2011). As will be seen, 'structure determination from powder diffraction data' (SDPD) can be considered as a routine, though not always straightforward, approach that has the advantage of dealing with a polycrystalline sample (in contrast to single-crystal diffraction, where a single crystal is not necessarily representative of the bulk material being handled in the pharmaceutical workflow). Many reviews of SDPD methodologies have now been published (Tremayne, 2004; Datta & Grant, 2004; David & Shankland, 2008; Cerny & Favre-Nicolin, 2007; Harris, 2012) and in particular, the IUCr Monograph on Crystallography 'Structure Determination from Powder Diffraction Data' (David et al., 2002) provides a 'powder sample to refined crystal structure' view of the process that is still valid today, despite some methodological advances in the field.

This article will look specifically at representative examples of pharmaceutical crystal structures (polymorphs, solvates, salts and cocrystals) solved using PXRD data and attempt to give the interested pharmaceutical scientist an insight into the principles underlying the various methodologies and their range of applicability.

2. Sample presentation and data collection for crystal structure determination

The outcome of any powder diffraction experiment that has crystal structure determination as its ultimate objective should be a diffraction pattern that is as representative of the underlying crystallographic phase(s) in the sample as possible. Whilst reflection is the most widely used instrumental PXRD geometry within the pharmaceutical industry, permitting easy sample presentation and rapid data collection for phase identification, it suffers from several disadvantages that render it non-ideal for crystal structure determination. In particular, the effect of sample transparency and preferred orientation introduce, respectively, shifts in the observed diffraction peak positions and systematic variations to the observed intensities (Dinnebier & Billinge, 2008). When crystal structure deter- mination is the ultimate aim, PXRD data are ideally collected in transmission with the sample loaded in a thin-walled glass capillary and rotated in the incident X-ray beam in order to minimize preferred orientation effects and give good powder averaging. On a well-aligned diffractometer, data collected in this fashion are likely to be highly representative of the underlying crystalline phase(s) in the sample. The advantages to industry of collecting PXRD data 'in-house' are consider- able and laboratory-based PXRD is capable of tackling complex problems (see, for example, x4.5 and x5). In cases where higher instrumental resolution or incident X-ray flux are required (e.g. very large unit cells, weak diffraction, extensively overlapping reflections) synchrotron X-ray sources offer an increasingly accessible option, with many such sources now offering postal-type services where the data collection aspects of the diffraction experiment are handled by facility staff.

Instrumentation and experimental considerations for both laboratory-based and synchrotron PXRD have been discussed, in detail, elsewhere (David et al., 2002). Whether collecting data in the laboratory, or at a synchrotron source, it is often advantageous to cool the sample in order to reduce

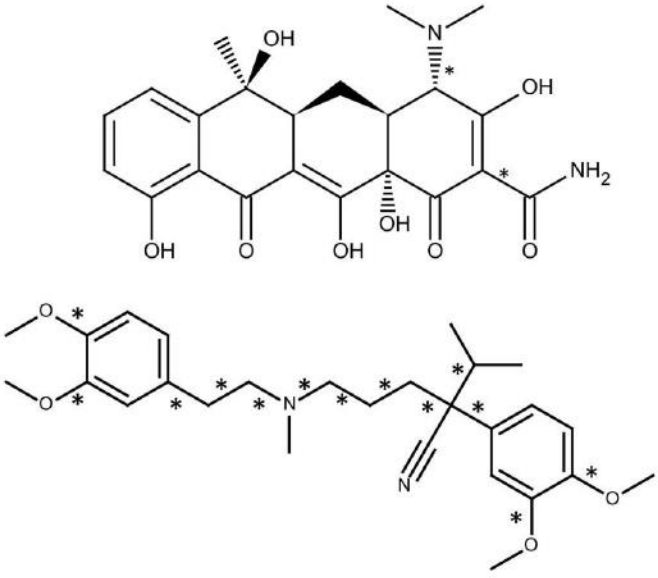

Figure 1
The molecular structures of tetracycline (upper) and verapamil (lower). Internal DoF (torsion angles that are free to rotate) are indicated by an asterisk (*). Assuming that the ring conformations are known, the structure of tetracycline (32 non-H atoms) can be described by 6 external DoF plus 2 internal DoF, whilst that of verapamil (33 non-H atoms) requires 6 external DoF plus 13 internal DoF. Thus, tetracycline is the much simpler problem to tackle using global optimization, as fewer variables need to be determined.

thermal vibration and so boost the intensity of the higher- angle reflections. Cooling of capillary samples to ca 100 K is conveniently achieved using devices that deliver a constant flow of temperature-stabilized nitrogen gas. Anisotropic thermal expansion of a lattice upon cooling can also be exploited to help with indexing and structure-factor extraction (Shankland, David & Sivia, 1997).

3. Structure complexity and powder diffraction

In single-crystal diffraction, structural complexity is normally thought of in terms of the number of non-H atoms in the asymmetric unit of the structure being studied, as this is the number of atom positions to be determined in the initial stages of structure solution. Whilst this definition is equally valid in the case of molecular SDPD, many problems are instead defined in terms of the number of degrees of freedom (DoF[1]) in the structure under study. This is a consequence of the way in which many molecular crystal structures are solved using global optimization methods that attempt to place a three- dimensional (3D) model of each component of the asymmetric unit at its correct position, orientation and conformation
within the unit cell (see x4.3). Fig. 1 shows these different metrics for two drug molecules with comparable numbers of non-H atoms, but markedly different conformational flex-
ibility. When assessing the complexity of structures that have been solved using SDPD, it is wise to consider both metrics.

Figs. 2-5 assess the development of SDPD over two decades, using information derived from the Cambridge Structural Database (CSD, Version 5.34 of November 2012; see Supplementary materials for CSD search criteria used; Allen, 2002). In his definitive summary of the CSD, Frank Allen stated that 'the number of structures determined from powder diffraction data is now 370, a number which is surely set to rise' (Allen, 2002). Fig. 2 shows this to be the case, with an average of 82 powder structures per year being added since 2002. Constituting only ca 1% of all crystal structures added in the same period, it shows SDPD to be a niche application for organic materials. That said, as SDPD is normally only brought to bear when single crystals are unavailable, it is undoubtedly a key tool for fully populating a crystallographic landscape. Fig. 3 shows that when assessed in terms of the number of atoms in the asymmetric unit of the crystal struc- ture, powder structures span a similar range to those solved by all methods, albeit in a much smaller overall number. This is encouraging, as it indicates that many of the problems that arise when single crystals cannot be obtained are tractable using SDPD methods. Fig. 4 shows the complexity of mol- ecular structures solved since 1990 and it is interesting to note that since the year 2000, the average number of asymmetric unit atoms in molecular crystal structures has stayed approximately constant at ca 52. In the case of SDPD, the steady rise in both the average and the maximum number of atoms reflects both method development and increasing ambition, with SDPD now well placed to tackle problems of ca 50 atom size. Fig. 5 shows the same structures as those contributing to Fig. 4, but cast in terms of the total number of DoF present in the structure. Again, it is clear that the average number of DoF in all structures reported has plateaued at just over 13 from the year 2000 onwards and that this is very
similar to the typical DoF that is now accessible to SDPD.

4. Approaches to SDPD

It is clear from the plots in x3 that the rise in the number of crystal structures solved from powder diffraction data began in earnest in the late 1990s and that their complexity has been slowly, but steadily, rising since that time. This can be attrib- uted to both the development and implementation of global optimization methods of structure determination and the continuing developments in modified direct methods of structure determination. The following sections describe both of these approaches and, in particular, highlight the reasons why global optimization methods have found favour in phar- maceutical crystal structure determination.

4.1. Key differences between single-crystal and powder diffraction data

The key differences between single-crystal and powder diffraction data have been discussed in detail elsewhere (David et al., 2002) and we only summarize them here in

[1] The DoF for a molecular organic molecule are subdivided into external DoF (i.e. three positional and three orientational) and internal (i.e. the number of torsion angles that are free to rotate). Covalent bond lengths and bond angles are generally treated as fixed well-defined quantities and so it is values for the DoF that must be determined in order to solve the crystal structure.

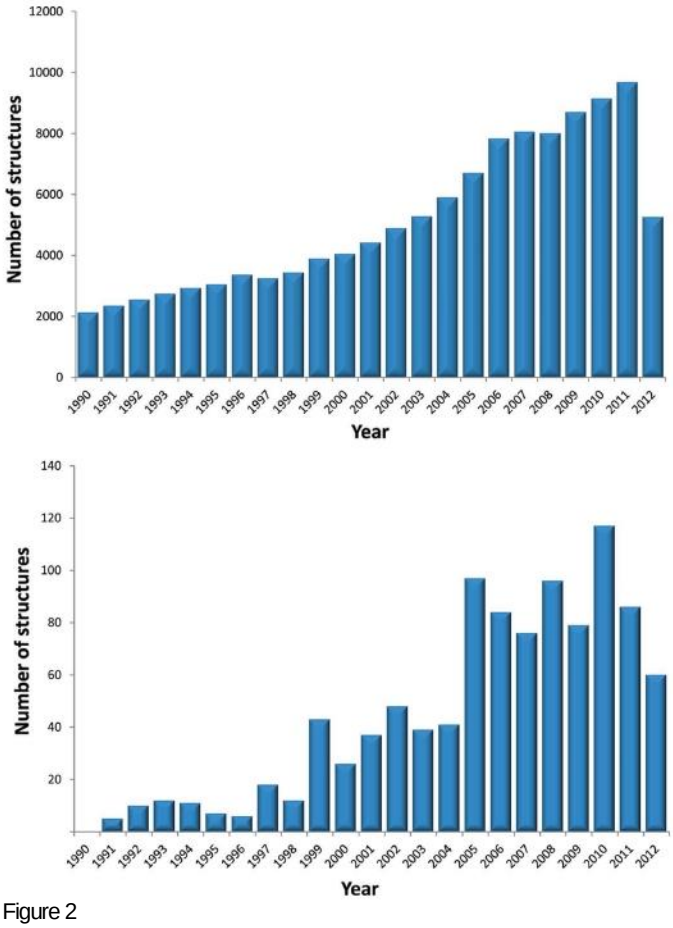

Figure 2
The number of molecular crystal structures deposited each year since 1990 in the Cambridge Structural Database (CSD). The upper plot is derived from all structures whilst the lower plot is derived from only powder structures. Note that the plot is based on the November 2012 release of the CSD and, therefore, the final total for 2012 will be higher than the value plotted here.

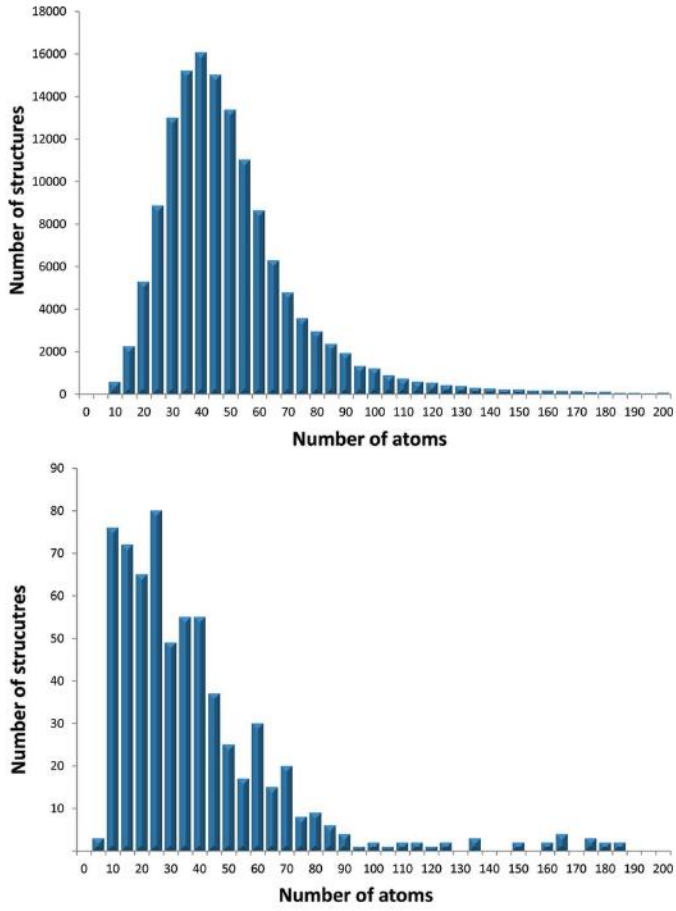

Figure 3
The number of molecular crystal structures present in the CSD, plotted as a function of the total number of atoms (including hydrogen) in the asymmetric unit of the structure. The upper plot is derived from all structures whilst the lower plot is derived from only powder structures.

Table 1 in terms of their impact upon structure solution. For molecular organic materials, typified by relatively low space-group symmetry and the absence of heavy atoms, it is acci- dental reflection overlap and the rapid fall off in scattering with increasing diffraction angle that leads to the relatively low information content of the powder diffraction pattern.

4.2. Conventional and modified direct methods

Direct methods, the lynchpin of single-crystal X-ray struc- ture determination, do not require any a priori knowledge of the connectivity or coordination of any of the atoms in the structure under study; connectivity is derived from the elec- tron-density map that is generated at the end of a structure- factor phasing process. The success of the phasing process and the clarity of the electron-density map is critically dependent upon the accuracy and resolution of those structure factors. As such, maps generated from conventional PXRD data are typically of poor quality and hence can be difficult to interpret. Of course, there are exceptions; when very high quality data are collected from a sharply diffracting sample, ideally containing some strongly scattering atoms, such as sulfur or chlorine, accurate structure factors may be obtained to near-atomic resolution and conventional direct methods of struc- ture determination (e.g. SHELXS; Sheldrick, 2008) then used to generate an interpretable map. The prototypical example is that of the crystal structure of cimetidine form A, solved from 1.273 A resolution synchrotron PXRD data (Cernik et al., ˚ 1991) using the SIR direct-methods package (Burla et al., 1989). Modified direct methods of structure determination have integrated the core of such direct methods into the process of extracting structure factors from PXRD data, with the aim of using partial structure information to improve the

Table 1
The key differences between single-crystal and powder diffraction data in terms of the information content that is relevant to solving molecular organic crystal structures.

	Single crystal	Powder
Number of reflections	Thousands	Hundreds
Minimum d-spacing	< 0.9A ˚	ca 1.3-1.5 A ˚
Accuracy of $\|F^2\|$	Very good	Very good to very poor*

Note: (*) $|F^2|$ estimates will normally be very good for non-overlapping reflections at low values of 2/ and increasingly poor at higher values of 2/ where diffraction is weaker and accidental reflection overlap is considerable.

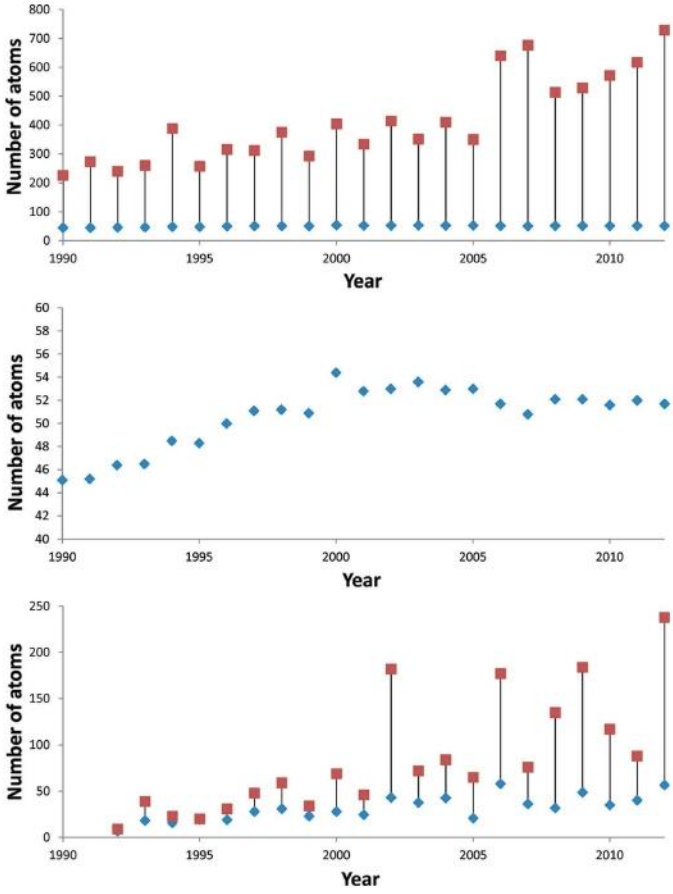

Figure 4
The mean (diamond) and maximum (square) of the total number of atoms (including hydrogen) in the asymmetric unit of molecular crystal structures deposited each year since 1990 in the CSD. The upper plot is derived from all structures; the middle plot shows an expanded view of the mean number of atoms for all structures; the lower plot is derived from only powder structures.

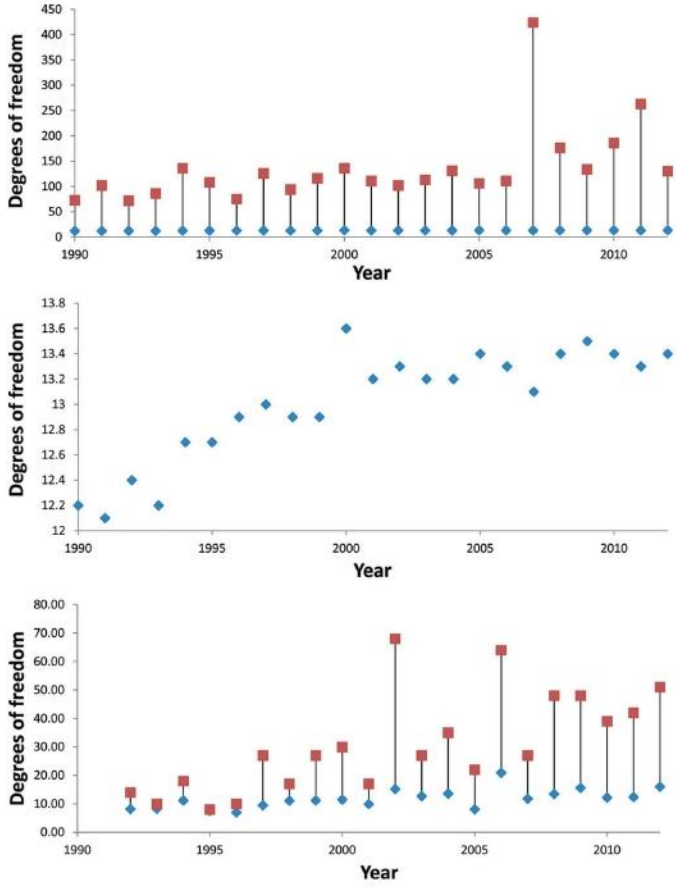

Figure 5
The mean (diamond) and maximum (square) total number of degrees of freedom in the asymmetric unit of molecular crystal structures deposited each year since 1990 in the CSD. The upper plot is derived from all structures; the middle plot shows an expanded view of the mean number of degrees of freedom for all structures; the lower plot is derived from only powder structures.

extracted structure factor intensity estimates. This, coupled with recent advances in electron density-map generation and interpretation, has relaxed the requirements for near-atomic resolution data and thus greatly extended the range of applicability of direct methods to powder diffraction data, obtained from both inorganic and organic materials. Many of these methods are implemented in the EXPO program (Altomare et al., 1999) from the University of Bari group, making it very well suited to dealing with laboratory-based PXRD data collected from typical molecular organic mate- rials.

4.3. Global optimization methods

Global optimization methods are a logical extension of trial-and-error methods of crystal structure determination. In trial-and-error methods, a model of the crystal structure under study is constructed[2] and the powder pattern calculated from that model is then compared to the observed powder pattern. If there is very good agreement between observed and calculated patterns (as assessed by, for example, a small profile $_^2$ value), then it can be concluded that the model is a good description of the underlying crystalline phase in the sample and that the crystal structure has been solved. Of course, for a typical molecular organic material, there is only an infinitesimally small chance of guessing the correct atomic positions first time; hence the trial-and-error approach, where the initial model is adjusted in such as way as to decrease the $_^2$. The problem of obtaining the lowest profile $_^2$ in fact equates to that of finding the global minimum of a multidimensional $_^2$ hypersurface that is a function of the DoF in the problem. This hypersurface is dominated by local stationary points and, in general, as the number of DoF in the optimization increases, it becomes more difficult for any given global optimization algorithm to locate the global minimum.

For the purposes of this article, it suffices to say that many different global optimization methods have been successfully brought to bear on this particular problem and the interested reader is referred to both the original articles and various reviews for details of how they work (Turner et al., 2000;

[2] An initial 3D model of each component in the asymmetric unit is typically obtained from existing crystal structures or via the use of molecular drawing/ modelling software that produces accurate energy-optimized 3D coordinates. The asymmetric unit components are then placed in the previously determined unit cell in order to construct a trial crystal structure.

Table 2
A summary of SDPD crystal structures, selected on the basis of pharmaceutical and historical interest. The corresponding molecular structures are shown in Fig. 6. N_{atom} = total number of atoms in the asymmetric unit; $N_{non\text{-}H}$ = total number on non-H atoms in the asymmetric unit; DoF = total number of degrees of freedom in the asymmetric unit.

Name	Entry in Fig. 6	Z^0	N_{atom}	$N_{non\text{-}H}$	DoF	Method	Software	
Salicylic acid	a	1	16	10	7	GS	P-RISCON	(Masciocchi et al., 1994)
Chlorothiazide	b	1	23	17	7	DM	MITHRIL94	(Shankland, David & Sivia, 1997)
Ibuprofen	c	1	33	15	10	GA	GAP	(Shankland et al., 1998)
l-Glutamic acid	d	1	19	10	10	LE	-	(Turner et al., 2000)
Remacemide nitrate	e	1	45	24	18	SA	DASH	(Markvardsen et al., 2002)
Tri-fi-peptide	f	1	94	41	23	SE+SA	Safe	(Brenner et al., 2002)
Capsaicin	g	1	49	22	15	HMC	-	(Markvardsen et al., 2005)
Baicalein	h	1	30	20	7	CDE-GA	-	(Chong & Tremayne, 2006)
Famotidine	i	1	35	20	13	PM	EXPO	(Burla et al., 2007)
Caffeine	j	5	120	70	30	SA	TOPAS	(Lehmann & Stowasser, 2007)
Captopril	k	1	29	14	10	MDM	EXPO	(Altomare et al., 2007)
Chlorothiazide	b	1	23	17	7	DM	SHELX	(Fernandes et al., 2008)
Cyheptamide	l	4	132	72	28	SA	DASH	(Florence et al., 2008)
Tolbutamide	m	1	36	18	13	PS	PeckCryst	(Feng et al., 2009)
Tolbutamide	m	1	36	18	13	GA	GEST	(Feng & Dong, 2007)
Capsaicin	g	1	49	22	15	LM	-	(Shankland et al., 2010)
Nifedipine	n	2	86	50	24	SA	ReX	(Bortolotti et al., 2009)
l-Arginine	o	2	52	24	25	GA	EAGER	(Courvoisier et al., 2012)
Amodiaquinium dichloride dihydrate	p	1	57	29	30	MDM	EXPO	(Altomare et al., 2012)
Vorinostat	q	1	39	19	16	SA/PT	FOX	(Puigjaner et al., 2012)
Amcinonide	r	2	142	72	20	SA	PSSP	(Pagola & Stephens, 2012)
Diphenhydramine hydrochloride	s	1	42	20	15	LM	TALP	(Vallcorba et al., 2012)
Verapamil hydrochloride	t	1	73	34	22	HBB-BC	EXPO	(Altomare, Corriero et al., 2013)
Zopiclone dihydrate	u	1	50	29	16	HY	EXPO	(Altomare, Cuocci et al., 2013)
Prilocaine	v	1	36	16	12	SA	PowderSolve	(Rietveld et al., 2013)

Key: CDE = cultural differential evolution; DM = direct methods; GA = genetic algorithm; GS = grid search; HBB-BC = hybrid big bang-big crunch; HMC = hybrid Monte Carlo; HY = hybrid methods; LE = Lamarckian evolution; LM = local minimization; MDM = modified direct methods; PM = Patterson methods; PS = particle swarm; PT = parallel tempering; SA = simulated annealing; SE = structure envelope.

Shankland, David & Csoka, 1997; Harris et al., 2004; Markvardsen et al., 2005; Chong & Tremayne, 2006; Altomare, Corriero et al., 2013; Shankland et al., 2010; Feng et al., 2009; Favre-Nicolin & Černý, 2002; Vallcorba et al., 2012; Pagola & Stephens, 2010; Feng & Dong, 2007; Le Bail, 2001; Brodski et al., 2005; Rapallo, 2009; Engel et al., 1999; David et al., 2006; Florence et al., 2005). Simulated annealing (Kirkpatrick et al., 1983) has proven to be the most widely used and successful method to date, largely because of its efficacy, ease-of-implementation in programmatic form and ease-of-use for the end user, i.e. most of the algorithm control parameters can be either preset or determined automatically, without user intervention. No single global optimization run is guaranteed to find the global minimum in a finite time. Accordingly, multiple runs, from randomized starting points, are generally required to increase the likelihood of locating the global minimum.

The majority of global optimization methods are amenable to parallelization, making it relatively straightforward and efficient to execute these multiple runs (Griffin et al., 2009a,b).

4.4. Other methods

A variety of other methods, including charge-flipping (Wu et al., 2006; Palatinus, 2013; Oszlanyi & Suto, 2008; Coelho, 2007) and molecular replacement (Von Dreele et al., 2000; Margio- laki & Wright, 2008; Noguchi et al., 2012), have been used to solve organic crystal structures from powder diffraction data. However, to date, these methods have not achieved the same impact on small-molecule SDPD as modified direct methods and global optimization methods. This is a consequence of the maturity of the latter approaches and the availability of software packages implementing them. However, in the specific case of charge flipping, the requirement for accurate structure factors to near-atomic resolution is a significant restriction when working with powder diffraction data.

4.5. Representative examples

Table 2 and Fig. 6 show a representative selection of pharmaceutical crystal structures that have been solved using SDPD techniques.

5. Specific examples of challenging structure determinations

5.1. Carbamazepine-indomethacin (1/1) cocrystal

The structure of a carbamazepine-indomethacin (1/1) cocrystal [CBZ-IND (1/1)], produced by cogrinding CBZ form III and -IND, was recently determined directly from PXRD data (Majumder et al., 2011). The structure determination was moderately challenging in terms of molecular complexity [Z^0 = 1, 71 atoms in the asymmetric unit, with 18 DoF (12 external plus 6 internal)], but was further complicated by the incomplete transformation of starting materials to cocrystal, resulting in a room-temperature laboratory PXRD pattern containing contributions from the cocrystal, CBZ form III and -IND. Knowing the positions of peak contributions from the previously determined crystal structures of the starting materials, it was possible to index the remaining peaks in the

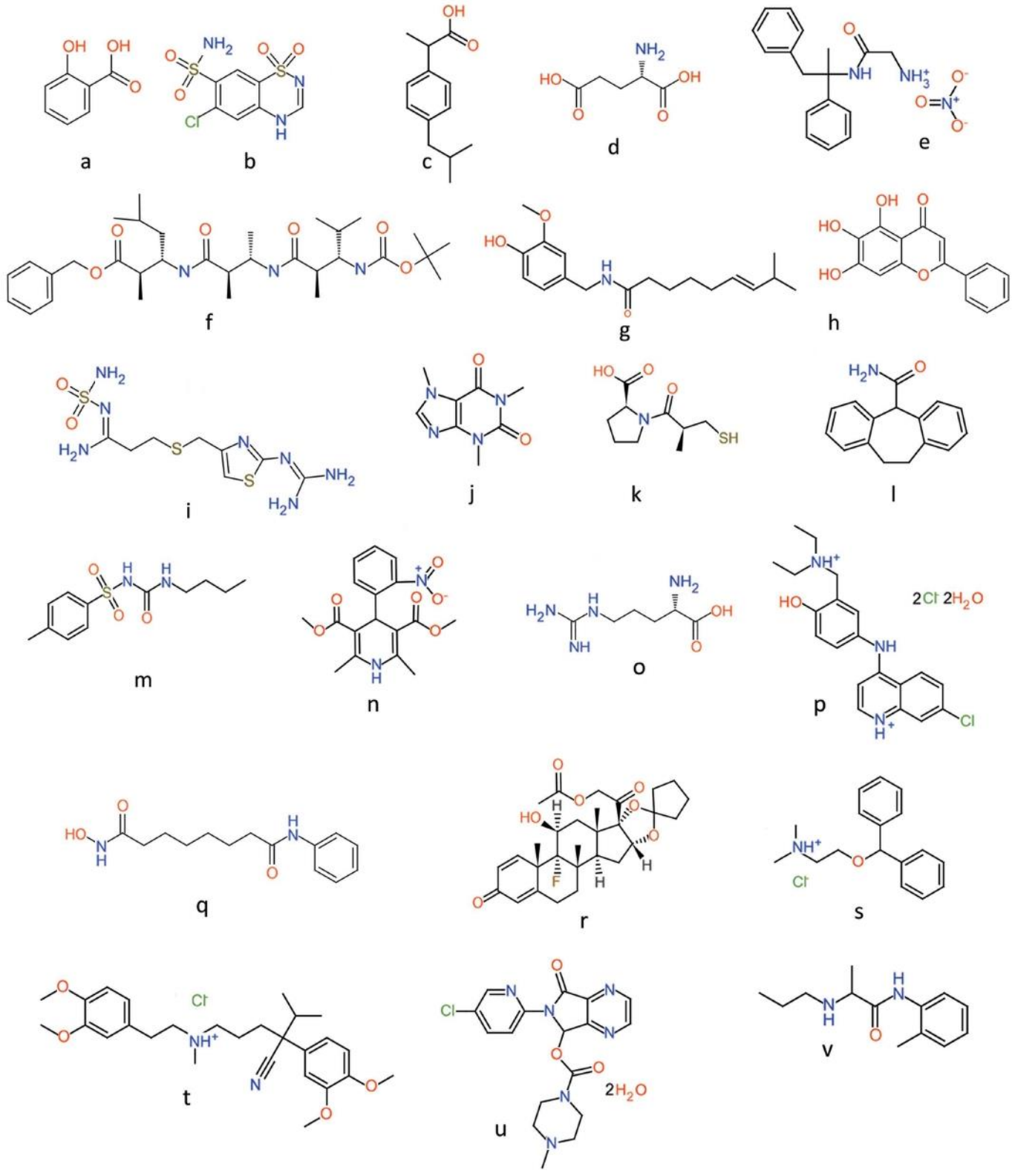

Figure 6
The molecular structures of the compounds listed in Table 2, obtained using MarvinSketch 'Name to Structure' (ChemAxon, 2011). A SMILES string for each structure, generated using MarvinSketch, is provided as Supplementary materials.

pattern and thus determine the unit cell of the novel cocrystal phase (Table 3). Thereafter, the CBZ form III and -IND contributions to the PXRD pattern were effectively eliminated by performing a Pawley refinement of the cocrystal unit cell in probable space group $P2_1/c$, whilst simultaneously carrying out a Rietveld refinement of the CBZ form III and

Table 3
CBZ-IND (1/1).

Instrument		Bruker D8 Advance with LynxEye detector
Geometry		Capillary (0.7 mm), transmission
Radiation		Cu Kff$_1$ (1.54056 A) ˚
Temperature		295 K
Scan range (^{1}) 2/	1	3-22 (2 s/0.017^1 step)
	2	22-40 (4 s/0.017^1 step)
	3	40-55 (15 s/0.017^1 step)
	4	55-70 (24 s/0.017^1 step)
Crystal system/space group		Monoclinic, P2$_1$/c
a, b, c (A) ˚		10.2447 (3), 29.148 (1), 10.2114 (3)
fi(^{1})		106.636 (2)
Volume (A^3) ˚		2921.6 (2)
SA runs		100 runs of 5 Â 10^6 SA moves; 4 solutions
Final R$_{wp}$ Pawley		1.58
Final R$_{wp}$ Rietveld		3.99
Asymmetric unit of crystal		

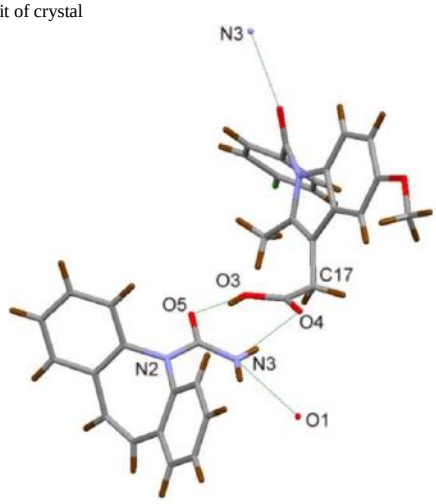

Table 4
CT-DMF2.

Instrument		Bruker D8 Advance with Braun detector
Geometry		Capillary (0.7mm), transmission
Radiation		Cu Kff$_1$ (1.54056 A) ˚
Temperature		295 K
Scan range (^{1}) 2/	1	4-15 (3 s/0.014^1 step)
	2	15-25 (6 s / 0.014^1 step)
	3	25-35 (14 s / 0.014^1 step)
	4	35-50 (32 s / 0.014^1 step)
	5	50-70 (64 s / 0.014^1 step)
Crystal system/space group		Monoclinic, P2$_1$/c
a, b, c (A) ˚		12.3586 (2), 8.5619 (2), 37.3043 (7)
fi(^{1})		92.8786 (13)
Volume (A^3 ˚		3942.30 (13)
SA runs		99 runs of 800 Â 10^6 SA moves; 4 solutions
Final R$_{wp}$ Pawley (2-65^1)		1.55
Final R$_{wp}$ Rietveld (2-65^1)		2.03
Asymmetric unit of crystal		

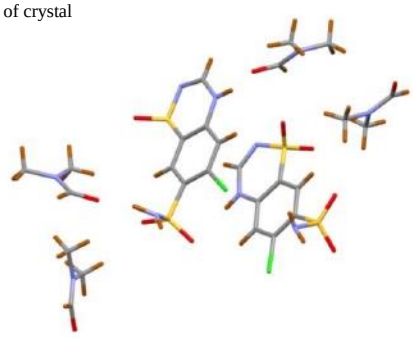

-IND crystal structures. The outcome of this process was a PXRD pattern containing only the scattering contribution from the cocrystal. Thereafter, SDPD using DASH (David et al., 2006) proceeded routinely. The solved structure was refined against the original PXRD data using a multiphase (cocrystal, CBZ form III, -IND) rigid-body-type Rietveld refinement in TOPAS (Coelho, 2003). This analysis highlights two very important points: (i) with grinding/milling experiments, where the production of crystals suitable for single-crystal diffraction is unlikely, it is still possible to obtain a crystal structure using SDPD; (ii) the presence of 'contam- inating' crystalline phases (starting materials, transformed starting materials) need not preclude high-quality crystal structure determination.

5.2. Chlorothiazide dimethylformamide solvate (CT-DMF2)

The crystal structure of a dimethylformamide (DMF) solvate of the diuretic compound chlorothiazide (CT) was solved directly from PXRD data (Fernandes et al., 2007). The compound, crystallized by slow evaporation of a saturated solution of DMF over a period of three months, was loaded into a 0.7 mm capillary along with a small amount of saturated DMF solution to prevent desolvation. PXRD data, collected at room temperature, indexed to a monoclinic unit cell of volume 3942 A^3 (Table 4), suggesting not only the presence of ˚ two molecules of DMF per CT, but also Z^0 = 2 [3]. Thus, the structure determination was extremely challenging in terms of molecular complexity [94 atoms in the asymmetric unit, with 42 DoF (36 external plus 6 internal)] and further complicated by the solvent contribution to the PXRD pattern background. Nevertheless, the structure was solved using DASH, with a large number of simulated annealing moves being employed in order to increase the likelihood of locating the global minimum in the complex structure solution space. With six independent fragments in the asymmetric unit, careful Riet- veld refinement of the DASH structure was required in order to ensure that the DMF molecules, in particular, were correctly positioned and oriented to give a chemically sensible hydrogen-bonding network.

6. Structure refinement

Rietveld refinement (Rietveld, 2010) aims to maximize the agreement between the calculated and observed powder diffraction profiles by adjusting the positions of the atoms from the initial solved crystal structure. As a consequence of the limited information content of the observed data, however, care must be taken to ensure that maximizing this agreement does not come at the expense of chemical sense. By way of example, the CBZ-IND (1/1) cocrystal structure

~~(Table 3) solved b~~y SA using data to 50^1 2/ (1.82 A resolution) ˚

[3] Estimated molecular volumes (Hofmann, 2002): V$_{CT}$ = 285 A^3; V$_{DMF}$ = 100 A^3; ˚ ˚ V$_{CT-DMF2}$ = 485 A^3. V$_{cell}$/V$_{CT-DMF2}$ = 8.1; hence Z = 8 and as the space group was ˚ determined to be P2$_1$/c, Z^0 = 2.

was refined against data to 65[1] 2/ (1.43 A resolution) using ˚ rigid-body descriptions of the CBZ and IND molecules in TOPAS (Coelho, 2003) in order to preserve their molecular geometries. The resultant high-quality fit to the full data range, coupled with the chemically reasonable geometry/crystal packing confirms the correctness of the CBZ-IND (1/1) cocrystal structure. The CT-DMF2 crystal structure refine- ment (Table 4) was approached slightly differently (individual atomic positions were refined, subject to a series of restraints on bond lengths, bond angles and group planarity), but the end result was the same, i.e. a good Rietveld fit to the observed data and a chemically reasonable CT-DMF2 crystal structure.

Looking beyond Rietveld refinement, and considering the increasingly large structures being solved using SDPD, peri- odic density functional theory calculations are being used increasingly to finalize features (particularly H-atom posi- tions) in the crystal structure that may not be particularly well defined by the diffraction data alone and also to identify energetically unrealistic structures (Bruening et al., 2011).

7. Publication

The final step before reporting a refined powder structure is to work-up the CIF to an acceptable standard. There are a number of helpful tools available, including MOGUL (Bruno et al., 2004) for checking geometry and enCIFer (Allen et al., 2004) for checking format compliance. A final check on the completed CIF is best carried out using the official IUCr structure-validation suite checkCIF/PLATON (Spek, 2009), accessible at http://journals.iucr.org/services/cif/checking/ checkfull.html. The powder CIF dictionary (pdCIF, http:// www.iucr.org/resources/cif/dictionaries/cif_pd) contains terms that are useful in describing PXRD-specific elements of a CIF, including diffraction profile data. Good examples of the correct usage of these terms can be found in the deposited CIFs that accompany submissions to IUCr journals and are freely available to download.

8. Outlook

There is no doubt that SDPD has made a small but highly significant contribution to the field of molecular crystal structure determination and that pharmaceutical sciences have benefitted as a result. Looking to the future, it appears electron crystallography is emerging as an exciting comple- ment to powder diffraction (McCusker & Baerlocher, 2013; Kolb et al., 2012) and that their combined use will further extend the range of applicability of SDPD to pharmaceuticals.

KS gratefully acknowledges the many long-standing collaborations and students that have contributed to the development of SDPD methods in the form of the DASH computer program, but in particular those with Bill David, Anders Markvardsen, Alastair Florence, Norman Shankland and the staff of the Cambridge Crystallographic Data Centre. We gratefully acknowledge the support of the STFC Centre for Molecular Structure and Dynamics for part-funding of MJS, CCDC and University of Reading for funding of EAK, EPSRC for funding of DSE and the University of Reading Chemical Analysis Facility for access to powder diffraction facilities.

References

Allen, F. H. (2002). Acta Cryst. B58, 380-388.
Allen, F. H., Johnson, O., Shields, G. P., Smith, B. R. & Towler, M. (2004). J. Appl. Cryst. 37, 335-338.
Altomare, A., Burla, M. C., Camalli, M., Carrozzini, B., Cascarano, G. L., Giacovazzo, C., Guagliardi, A., Moliterni, A. G. G., Polidori, G. & Rizzi, R. (1999). J. Appl. Cryst. 32, 339-340.
Altomare, A., Camalli, M., Cuocci, C., Giacovazzo, C., Moliterni, A. G. G. & Rizzi, R. (2007). J. Appl. Cryst. 40, 344-348.
Altomare, A., Corriero, N., Cuocci, C., Moliterni, A. & Rizzi, R. (2013). J. Appl. Cryst. 46, 779-787.
Altomare, A., Cuocci, C., Giacovazzo, C., Moliterni, A. & Rizzi, R. (2012). J. Appl. Cryst. 45, 789-797.
Altomare, A., Cuocci, C., Moliterni, A. & Rizzi, R. (2013). J. Appl. Cryst. 46, 476-482.
Bortolotti, M., Lutterotti, L. & Lonardelli, I. (2009). J. Appl. Cryst. 42, 538-539.
Brenner, S., McCusker, L. B. & Baerlocher, C. (2002). J. Appl. Cryst. 35, 243-252.
Brittain, H. G. (2001). Spectroscopy, 16, 14.
Brodski, V., Peschar, R. & Schenk, H. (2005). J. Appl. Cryst. 38, 688-693.
Bruening, J., Alig, E., van de Streek, J. & Schmidt, M. U. (2011). Z. Kristallogr. 226, 476-482.
Bruno, I. J., Cole, J. C., Kessler, M., Luo, J., Motherwell, W. D. S., Purkis, L. H., Smith, B. R., Taylor, R., Cooper, R. I., Harris, S. E. & Orpen, A. G. (2004). J. Chem. Inf. Comput. Sci. 44, 2133-2144.
Burla, M. C., Caliandro, R., Carrozzini, B., Cascarano, G. L., De Caro, L., Giacovazzo, C., Polidori, G. & Siliqi, D. (2007). J. Appl. Cryst. 40, 834-840.
Burla, M. C., Camalli, M., Cascarano, G., Giacovazzo, C., Polidori, G., Spagna, R. & Viterbo, D. (1989). J. Appl. Cryst. 22, 389-393.
Cernik, R. J., Cheetham, A. K., Prout, C. K., Watkin, D. J., Wilkinson, A. P. & Willis, B. T. M. (1991). J. Appl. Cryst. 24, 222-226.
Cerny, R. & Favre-Nicolin, V. (2007). Z. Kristallogr. 222, 105-113.
ChemAxon (2011). MarvinSketch. ChemAxon Kft., Budapest, Hungary.
Chieng, N., Rades, T. & Aaltonen, J. (2011). J. Pharm. Biomed. Anal. 55, 618-644.
Chong, S. Y. & Tremayne, M. (2006). Chem. Commun. pp. 4078-4080.
Coelho, A. (2003). TOPAS User Manual. Bruker AXS GmbH, Karlsruhe, Germany.
Coelho, A. A. (2007). Acta Cryst. A63, 400-406.
Courvoisier, E., Williams, P. A., Lim, G. K., Hughes, C. E. & Harris, K. D. M. (2012). Chem. Commun. 48, 2761-2763.
Datta, S. & Grant, D. J. W. (2004). Nature Rev. Drug Discov. 3, 42-57. David,
W. I. F. & Shankland, K. (2008). Acta Cryst. A64, 52-64.
David, W. I. F., Shankland, K., McCusker, L. B. & Baerlocher, C. (2002). Editors. Structure Determination from Powder Diffraction Data. Oxford University Press.
David, W. I. F., Shankland, K., van de Streek, J., Pidcock, E., Motherwell, W. D. S. & Cole, J. C. (2006). J. Appl. Cryst. 39, 910-915.
Dinnebier, R. E. & Billinge, S. J. L. (2008). Powder Diffraction: Theory and Practice, pp. 1-19. Cambridge: RSC Publishing.
Engel, G. E., Wilke, S., Konig, O., Harris, K. D. M. & Leusen, F. J. J. (1999). ¨ J. Appl. Cryst. 32, 1169-1179.
Favre-Nicolin, V. & Cerny, R. (2002). J. Appl. Cryst. 35, 734-743.
Feng, Z. J. & Dong, C. (2007). J. Appl. Cryst. 40, 583-588.
Feng, Z. J., Dong, C., Jia, R. R., Deng, X. D., Cao, S. X. & Zhang, J. C. (2009). J. Appl. Cryst. 42, 1189-1193.
Fernandes, P., Shankland, K., David, W. I. F., Markvardsen, A. J., Florence, A. J., Shankland, N. & Leech, C. K. (2008). J. Appl. Cryst. 41, 1089-1094.
Fernandes, P., Shankland, K., Florence, A. J., Shankland, N. & Johnston, A. (2007). J. Pharm. Sci. 96, 1192-1202.
Florence, A. J. (2009). In Polymorphism in Pharmaceutical Solids, 2nd ed., edited by H. G. Brittain. New York: Informa Healthcare.

Florence, A. J., Shankland, K., Gelbrich, T., Hursthouse, M. B., Shankland, N., Johnston, A., Fernandes, P. & Leech, C. K. (2008). CrystEngComm, 10, 26-28.
Florence, A. J., Shankland, N., Shankland, K., David, W. I. F., Pidcock, E., Xu, X., Johnston, A., Kennedy, A. R., Cox, P. J., Evans, J. S. O., Steele, G., Cosgrove, S. D. & Frampton, C. S. (2005). J. Appl. Cryst. 38, 249-259.
Griffin, T. A. N., Shankland, K., van de Streek, J. & Cole, J. (2009a). J. Appl. Cryst. 42, 356-359.
Griffin, T. A. N., Shankland, K., van de Streek, J. & Cole, J. (2009b). J. Appl. Cryst. 42, 360-361.
Harris, K. D. M. (2012). Advanced X-ray Crystallography, edited by K. Rissanen, pp. 133-177. Berlin: Springer.
Harris, K. D. M., Habershon, S., Cheung, E. Y. & Johnston, R. L. (2004). Z. Kristallogr. Cryst. Mater. 219, 838-846.
Hofmann, D. W. M. (2002). Acta Cryst. B58, 489-493.
Ivanisevic, I., McClurg, R. B. & Schields, P. J. (2010). In Pharmaceutical Sciences Encyclopedia, edited by S. C. Gad. New York: John Wiley & Sons Inc.
Kirkpatrick, S., Gelatt, C. D. & Vecchi, M. P. (1983). Science, 220, 671-680.
Kolb, U., Shankland, K., Meshi, L., Avilov, A. & David, W. I. F. (2012). In Uniting Electron Crystallography and Powder Diffraction. Dordrecht: Springer.
Le Bail, A. (2001). Epdic 7: European Powder Diffraction, Parts 1 and 2, edited by R. Delhez & E. J. Mittemeijer, pp. 65-70. Zurich: Trans Tech Publications.
Lehmann, C. W. & Stowasser, F. (2007). Chem. Eur. J. 13, 2908-2911.
Lemmerer, A., Bernstein, J., Griesser, U. J., Kahlenberg, V., Toebbens, D. M., Lapidus, S. H., Stephens, P. & Esterhuysen, C. (2011). Chem. Eur. J. 17, 13445-13460.
Majumder, M., Buckton, G., Rawlinson-Malone, C., Williams, A. C., Spillman, M. J., Shankland, N. & Shankland, K. (2011). CrystEngComm, 13, 6327-6328.
Margiolaki, I. & Wright, J. P. (2008). Acta Cryst. A64, 169-180.
Markvardsen, A. J., David, W. I. F. & Shankland, K. (2002). Acta Cryst. A58, 316-326.
Markvardsen, A. J., Shankland, K., David, W. I. F. & Didlick, G. (2005). J. Appl. Cryst. 38, 107-111.

Masciocchi, N., Bianchi, R., Cairati, P., Mezza, G., Pilati, T. & Sironi, A. (1994). J. Appl. Cryst. 27, 426-429.
McCusker, L. B. & Baerlocher, C. (2013). Z. Kristallogr. 228, 1-10.
Morissette, S. L., Almarsson, O., Peterson, M. L., Remenar, J. F., Read, M. J., Lemmo, A. V., Ellis, S., Cima, M. J. & Gardner, C. R. (2004). Adv. Drug Deliv. Rev. 56, 275-300.
Noguchi, S., Miura, K., Fujiki, S., Iwao, Y. & Itai, S. (2012). Acta Cryst. C68, o41-o44.
Oszlanyi, G. & Suto, A. (2008). Acta Cryst. A64, 123-134.
Pagola, S. & Stephens, P. W. (2010). J. Appl. Cryst. 43, 370-376. Palatinus, L. (2013). Acta Cryst. B69, 1-16.
Pagola, S. & Stephens, P. W. (2012). CrystEngComm, 14, 5349-5354.
Puigjaner, C., Barbas, R., Portell, A., Valverde, I., Vila, X., Alcobe, X., Font-Bardia, M. & Prohens, R. (2012). CrystEngComm, 14, 362-365.
Randall, C., Rocco, W. & Ricou, P. (2010). Am. Pharm. Rev. 13, 52-59. Rapallo, A. (2009). J. Chem. Phys. 131, 044113.
Rietveld, H. M. (2010). Z. Kristallogr. 225, 545-547.
Rietveld, I. B., Perrin, M.-A., Toscani, S., Barrio, M., Nicolai, B., Tamarit, J.-L. & Ceolin, R. (2013). Mol. Pharm. 10, 1332-1339.
Shankland, K., David, W. I. F. & Csoka, T. (1997). Z. Kristallogr. Cryst. Mater. 212, 550-552.
Shankland, K., David, W. I. F., Csoka, T. & McBride, L. (1998). Int. J. Pharm. 165, 117-126.
Shankland, K., David, W. I. F. & Sivia, D. S. (1997). J. Mater. Chem. 7, 569-572.
Shankland, K., Markvardsen, A. J., Rowlatt, C., Shankland, N. & David, W. I. F. (2010). J. Appl. Cryst. 43, 401-406.
Sheldrick, G. M. (2008). Acta Cryst. A64, 112-122. Spek, A. L. (2009). Acta Cryst. D65, 148-155.
Tremayne, M. (2004). Philos. Trans. R. Soc. London Ser. Math. Phys. Eng. Sci. 362, 2691-2707.
Turner, G. W., Tedesco, E., Harris, K. D. M., Johnston, R. L. & Kariuki, B. M. (2000). Chem. Phys. Lett. 321, 183-190.
Vallcorba, O., Rius, J., Frontera, C. & Miravitlles, C. (2012). J. Appl. Cryst. 45, 1270-1277.
Von Dreele, R. B., Stephens, P. W., Smith, G. D. & Blessing, R. H. (2000). Acta Cryst. D56, 1549-1553.
Wu, J., Leinenweber, K., Spence, J. C. H. & O'Keeffe, M. (2006). Nat. Mat. 5, 647-652.